Proprioceptive-Inertial Autonomous Locomotion for Articulated Robots

Francesco Ruscelli[1], Guillaume Sartoretti[1], Junyu Nan[1], Zhixin Feng[1], Matthew Travers[1] and Howie Choset[1]

***Abstract*— Inspired by the ability of animals to rely on proprioception and vestibular feedback to adapt their gait, we propose a modular framework for autonomous locomotion that relies on force sensing and inertial information. A first controller exploits anti-compliance, a new application of positive force feedback, to quickly react against obstacles upon impact. We hypothesize that, in situations where a robot experiences occasional impacts with the environment, anti-compliance can help negotiate unknown obstacles, similar to biological systems where positive feedback enables fast responses to external stimuli. A novel parallel controller, based on a bi-stable dynamical system, continuously adjusts the robot's direction of locomotion, and reverts it in reaction to major swerves. We present experimental results, demonstrating how our framework allows a snake robot to autonomously locomote through a row of unevenly-spaced obstacles. Finally, we extend our proprioceptive controller to legged locomotion, showing how a hexapod robot can adapt its motion to climb over obstacles.**

I. Introduction

Many mobile robots experience frequent impacts with the environment during locomotion in challenging terrains. Articulated robots, such as crawling or walking robots, can leverage crucial information about their surrounding, obtained through these interactions, in order to adapt their gait without losing a given direction of motion. In particular, a snake robot using a sidewinding gait [1], [2] to navigate cuts a wide path through the environment, making it more difficult to fit through narrow openings and negotiate obstacles without losing its orientation. In this work we propose a new framework that only relies on on-board sensors, such as force sensors and Inertial Measurement Units (IMUs), for the autonomous locomotion of articulated robots in challenging environments. Our contribution is twofold: we introduce anti-compliance, as an extension of shape-based compliance [3], [4] to overcome impacts with obstacles, and we propose a new inertial controller to maneuver a snake robot through obstacles during sidewinding. Finally, we implement the proposed framework both on a snake robot and a hexapod robot to overcome obstacles, by relying solely on inertial and proprioceptive feedback. The robots are not equipped with any camera: our proprioceptive-inertial method is sufficient to enable effective locomotion. However, it could be used along with a vision system to improve the robot navigation, providing a low level controller capable of dealing with smaller obstacles upon impacts.

[1]F. Ruscelli, G. Sartoretti, J. Nan, Z. Feng, M. Travers and H. Choset are with the Robotics Institute at Carnegie Mellon University, Pittsburgh, PA 15213, USA. {francesco.ruscelli}@studio.unibo.it, {gsartore, jnan1, zhixinf}@andrew.cmu.edu, {mtravers@andrew, choset@cs}.cmu.edu

More specifically, we propose a biologically-inspired modular framework, which enables autonomous locomotion without any a-priori knowledge of the environment. Our approach is inspired by the combined use of the proprioceptive and vestibular systems in animal locomotion [5], [6], and relies on force sensors to feel the external environment, as well as IMUs to estimate the robot's orientation and correct its motion. Specifically, the robot locomotion is governed by two different subsystems:

1. *Proprioceptive shape adaptation* resembles animal proprioceptive reflexes that allow to adapt locomotion in response to contacts with their surroundings [7], [8]. It relies on a motion parametrization to link relevant parameters to external forces, to adapt and overcome obstacles by relying on positive force feedback. Effectively, positive feedback grants rudimentary reflexes to the robot, thus providing fast responses to external stimuli [9], [10]. Instead of a planned action or movement, which would require some a-priori knowledge of its surroundings, the robot responds by reflex when the body impacts an impediment. We implement this new technique by exploiting a modified version of the shape-based locomotion framework [3], [4] to focus on anti-compliance, a new application of positive feedback control. Our hypothesis is that, in cases where the robot's locomotion only results in occasional impacts with the environment, the use of anti-compliance can help negotiate unknown obstacles. Since our strategy is reflex-based and does not have a planning phase, the behaviour is not globally optimal with respect to overcoming obstacles, We expect that amplified reactions will not affect the stability of the gait, since the forces sensed return to nominal levels after a collision and normal locomotion can resume. As a result, this ensures that the energy exchanged between environment and robot during a physical interaction won't build up, decreasing after each impact and preventing damages to the body.

2. *Inertial motion adaptation* allows a robot to follow a constant direction of motion without getting diverted by obstacles. It adapts the robot's motion in response to changes in its orientation, by adjusting relevant parameters of the motion parametrization. This subsystem is divided into two parallel controllers. The first controller corrects minor orientation errors by steering the robot back to the desired course. The second, a new approach inspired by recent results in gait transitions [11], is a bi-stable dynamical system that handles major swerves by fluidly switching between different behaviours, i.e. inverting the robot's motion.

The paper is organized as follows: in Section II, we build on the shape-based locomotion framework [3] and propose a proprioceptive shape adaptation controller that

relies on positive force feedback. Section III introduces our controller for inertial-based motion adaptation. In Section IV, we experimentally validate our framework on a snake robot. Section V extends the proposed proprioceptive controller to legged locomotion, and presents experimental results on a hexapod robot. Finally, conclusions and future works are discussed in Section VI.

II. Proprioceptive shape adaptation

In this section, we detail how the robot's motion is adapted in response to external forces from the environment. To illustrate our approach, we consider the example of a highly-redundant snake robot performing a sidewinding gait. The robot's motion can be parameterized as a serpenoid curve [12], [13]. Building on the shape-based framework for locomotion [3], we show how to adapt relevant motion parameters with respect to external forces and to the current configuration of the robot.

A. Serpenoid curves

A snake robot is composed of N identical links, whose cyclic movements provide the robot with the ability to move. The resulting gaits are parameterized by two independent sine waves, which define joint trajectories for locomotion. One governs the links in the lateral plane, the other controls the links in the dorsal plane:

$$\begin{cases} \theta_i^{lat}(t) \;=\; \phi^{lat} + A^{lat}\sin(\omega_S^{lat} s_i^{lat} - \omega_T^{lat} t) \\ \theta_i^{dor}(t) \;=\; \phi^{dor} + A^{dor}\sin(\omega_S^{dor} s_i^{dor} - \omega_T^{dor} t + \sigma), \end{cases} \tag{1}$$

where the first equation refers to the lateral plane while the second one to the dorsal plane. θ_i^{lat} and θ_i^{dor} are the commanded joint angles, ϕ^{lat} and ϕ^{dor} the angular offset, A^{lat} and A^{dor} the amplitude of the curvatures, σ the phase shift between the two sine waves. ω_T^{lat} and ω_T^{dor} are the temporal frequencies, while ω_S^{lat} and ω_S^{dor} define the spatial frequencies, which determines the number of waves on the snake robot's body. $s_i^{lat} \in \{0, 2\cdot l_s, \ldots, N\cdot l_s\}$ and $s_i^{dor} \in \{l_s, 3\cdot l_s, \ldots, (N-1)\cdot l_s\}$ describe the position of each module with respect to the head, where l_s is the length of one module. These parameters can be tuned to define a wide range of gaits [14]. In particular, sidewinding is achieved by setting $\phi^{lat} = \phi^{dor} = 0$, $\omega_T^{lat} = \omega_T^{dor}$ and $\sigma = \frac{3}{4}\pi$.

B. Shape-based framework for locomotion

In hyper-redundant robots shape-based control is used to improve tractability of the system by reducing its dimensionality [3]. This approach uses shape functions, $h : \Sigma \to \mathbb{R}^N$, to determine joint angles $\theta^{\{dor,lat\}}(t)$ as a function of a small number of parameters, instead of governing each degree-of-freedom in $\mathbb{R}^N$. The controlled parameters lie in a lower dimension space, the *shape space* Σ.

In this work, the serpenoid curve Eq.(1)'s amplitude and spatial frequency are dynamically updated. The shape function h links these parameters while all others are fixed:

$$\begin{array}{rcl} h: & & \Sigma = \mathbb{R}^2 \mapsto \mathbb{R}^N \\ h_i^{lat}(A(t),\omega_S(t)) & = & \theta_0 + A(t)\sin\left(\omega_S(t)\, s_i - \omega_T\, t\right) \\ h_i^{dor}(A(t),\omega_S(t)) & = & \theta_0 + A(t)\sin\left(\omega_S(t)\, s_i - \omega_T\, t + \sigma\right). \end{array} \tag{2}$$

C. Anti-compliance

We extend the shape-based compliant framework presented in [3] by introducing *anti-compliance*. Similarly to [3], $A(t)$ and $\omega_S(t)$ (now time-dependent) are determined by the output of an admittance controller [15]. This controller allows the robot to adapt these two serpenoid parameters with respect to a set of external torques $\tau_{ext}(t) \in \mathbb{R}^N$, that are measured at each joint along the snake's body. The admittance controller for $\beta = \big(A(t), \omega_S(t)\big)^T$ reads:

$$M\,\ddot{\beta}(t) + B\,\dot{\beta}(t) + K\,(\beta(t) - \beta_0) = F(t), \tag{3}$$

where $M, B, K \in \mathbb{R}^{2\times 2}$ respectively represent the effective mass, damping and spring constant matrices of the system; $F(t)$ is a mapping of the external torques $\tau_{ext}(t)$ in the shape space Σ. In the absence of external forces, the control parameters will converge back to their nominal values β_0.

The shape function Eq.(2) is used to map the external torques measured along the snake's body to Σ, by means of the associated Jacobian matrix $J(h) \in \mathbb{R}^{2\times N}$:

$$J(h) = \begin{pmatrix} \frac{\partial h_1(A,\omega_S)}{\partial A} & \cdots & \frac{\partial h_N(A,\omega_S)}{\partial A} \\ \frac{\partial h_1(A,\omega_S)}{\partial \omega_S} & \cdots & \frac{\partial h_N(A,\omega_S)}{\partial \omega_S} \end{pmatrix}. \tag{4}$$

As opposed to [3], where the admittance controller (3) was used to stabilize the system, i.e., adapt the robot's shape to comply to external forces, we propose here anti-compliance, which is based on the concept of positive feedback: reacting reflexes are activated and enhanced by impacts, resulting in the snake pushing against obstacles while adapting its shape.

That is, in our case, external torques are mapped from the joint space to the shape space, via:

$$F(t) = -\,J(h)|_{(A(t),\omega_S(t))} \cdot \tau_{ext}(t). \tag{5}$$

We hypothesize that anti-compliance is beneficial to occasional obstacle negotiation during locomotion tasks. In gaits that aren't obstacle aided, such as the sidewinding gait, the propelling action provided by the gait together with the shape-deforming effect given by the anti-compliance controller allow an effective locomotion through obstacles. That is, we expect positive feedback to allow the robot to react against an obstacle, rather than comply to it: when a quick reaction is not enough to overcome an impediment, the snake remains in contact with it while accordingly deforming its shape. This behavior should enable a robot to obtain more information about the obstacle via force sensing, e.g., dimensions or shape, and better adapt its locomotion to overcome it.

D. Decentralized Control

Recent result have shown that a decentralized control is highly preferable for a snake moving through unknown obstacles [4]: it allows different portions of the snake's body to react independently to external disturbances, which results in a more effective locomotion. We hypothesize that the advantages of a decentralized control holds for a snake robot autonomously traveling in a unknown terrain, and we extend previous work to take into consideration anti-compliance.

Decentralized control splits the backbone of the snake into independent portions of neighboring joints. Thus, it couples joints along the snake's body using activation windows: each one has specific motion parameters which only respond to torques applied to joints belonging to the same activation window. This framework resembles biological reflexes when used in synergy with anti-compliance: muscle contractions are produced by local force feedbacks [10].

Activation windows, together with their relatives motion parameters, are defined by using sigmoid functions:

$$\beta(s,t) = \sum_{j=1}^{W} \beta_{s,j}(t) \left[\frac{1}{1+e^{m(s_{j,s}-s)}} + \frac{1}{1+e^{m(s-s_{j,e})}} \right] \quad (6)$$

where m controls the steepness of the windows, W is the number of windows, and $\beta_{s,j}(t)$ the values of the serpenoid parameters in window j at position s along the backbone of the snake. Window j spans the backbone of the robot over $[s_{j,s}; s_{j,e}] \subset [0;1]$.

Here, we aim to experimentally demonstrate how different degrees of centralization of the shape parameters result in a more effective and reliable motion. Specifically, we let spatial frequency be fully centralized, such that any force felt by the snake robot changes the whole body's spatial frequency parameter. In particular, when the robot contacts several obstacles simultaneously, we expect this centralization to allow the robot to adapt its wavelength to fit between obstacles. We let the amplitude be variably decentralized, depending on the spatial frequency of the serpenoid curve (i.e., how many waves on the snake). Amplitude windows are anchored between node points of the sine wave. Moreover, the windows that define the independent segments are not fixed to the snake's backbone. Instead, they are moved along the snake at the same velocity as the serpenoid wave, in order to pass information back down the body. We expect this backward-propagation mechanism to help the snake sidewind through obstacles, as soon as the first portion of the snake has found a way through an opening.

III. Inertial motion adaptation

In this section, we detail our approach to adapt the robot's locomotion in response to changes in its orientation caused by collisions with external obstacles. Exploiting the parameterized motion of a snake robot, we introduce two controllers that link the relevant parameters to the instantaneous direction of locomotion of the snake in order to i) continuously correct its heading and ii) reverse its motion when it has drastically diverted from its nominal direction.

A. Heading adjustment

The first inertial-based controller corrects small variations in the snake robot's direction of motion by exploiting differential sidewinding [1] in order to continuously adjust the snake's heading. Specifically, the temporal frequency $\omega_{T,s}(t)$ $(0 \leq s \leq 1)$ of each lateral joint along the backbone of the snake is adapted based on the current snake's heading $h(t)$:

$$\omega_{T,s}(t) = s \cdot (1 - \cos[h(t)]) \cdot \omega_T, \quad (7)$$

with ω_T the nominal temporal frequency of the snake. In our case, we only apply to the front or back half of the snakes, in order to steer the snake back to its nominal direction of motion. We introduce a minimal temporal frequency $\omega_{T,s}(t)$, so to prevent joints from completely stopping their motion.

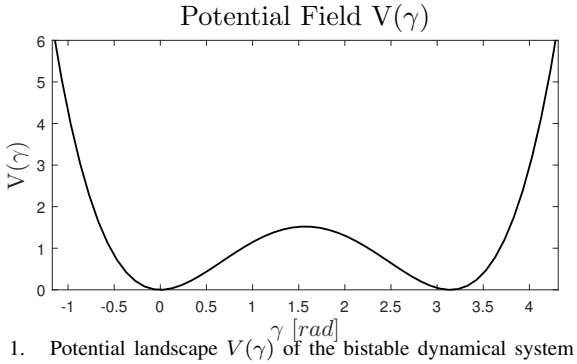

Fig. 1. Potential landscape $V(\gamma)$ of the bistable dynamical system with two attractors at $x = 0$ and $x = \pi$.

B. Direction reversal

The reversal is the core controller of the snake's motion orientation. While traveling forward, the snake robot may push against an obstacle, revolve around it and end up oriented in the opposite direction. In such case, changing the phase offset σ from Eq.(1) smoothly reverses the snake's motion to resume locomotion in the nominal direction. In this work, we consider an additional phase offset $\gamma(t) \in [0; 2\pi]$ in the dorsal serpenoid curve:

$$\begin{cases} \theta_i^{lat} = A^{lat} \sin(\omega_S^{lat} s_i^{lat} - \omega_T^{lat} t) \\ \theta_i^{dor} = A^{dor} \sin(\omega_S^{dor} s_i^{dor} - \omega_T^{dor} t + \sigma + \gamma(t)). \end{cases} \quad (8)$$

When $\gamma(t) = 0$, the snake sidewinds forward, while $\gamma = \pi$ produces backwards sidewinding.

We build a dynamical system in which the offset $\gamma(t)$ is updated with respect to the snake's heading $h(t)$. To this end, we build a simple bistable potential landscape $V(x)$, consisting of two attractive wells, where $\gamma_0 = 0$ and $\gamma_2 = \pi$ are the two attractors, while $\gamma_1 = \frac{\pi}{2}$ is the unstable saddle equilibrium point between the two wells. The potential landscape $V(\gamma)$ is depicted in Figure 1, and its associated gradient reads:

$$\frac{\mathrm{d}V}{\mathrm{d}\gamma}(\gamma) = \prod_{i=0}^{2} (\gamma - \gamma_i)\, dx. \quad (9)$$

In this landscape, we link the heading $h(t)$ and the offset $\gamma(t)$ by the linear dynamical system:

$$\dot{\gamma} = -K_b \cdot \frac{\mathrm{d}V}{\mathrm{d}x}(\gamma(t)) + K_h \cdot (h(t) - \gamma(t)), \quad (10)$$

where $K_b, K_h \in \mathbb{R}$ are scalar weights. Initially, $\gamma(0) = \gamma_0 = 0$, corresponding to forward sidewinding. Minor perturbations of the heading $h(t)$ of the snake do not affect the parameter $\gamma(t)$, which is attracted by the first stable point. However, since the heading and $\gamma(t))$ are linked by the second part of Eq.(10), if the heading $h(t)$ changes drastically, it drags the offset $\gamma(t)$ along, eventually pulling it past the unstable point γ_1. As soon as $\gamma(t) > \gamma_1$, it starts being attracted by the second stable point γ_2, inverting the snake robot motion's to backward sidewinding. A video detailing the evolution of the snake's offset $\gamma(t)$ and the heading $h(t)$ in the bistable potential Eq.(9), during a reversal maneuver can be seen online at `https://goo.gl/b489PX`.

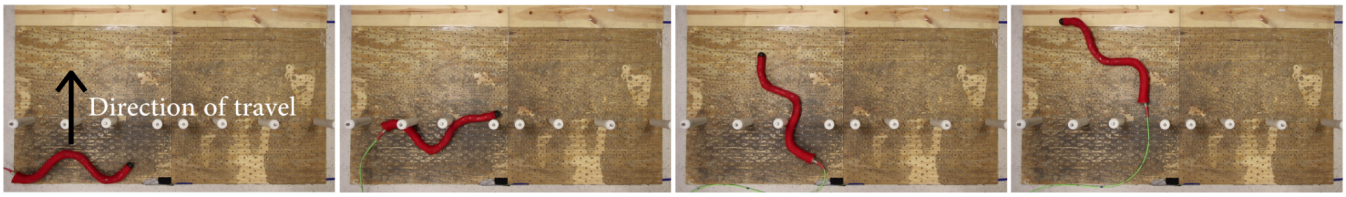

Fig. 2. Sequence of frames of the snake robot passing through a row of pegs in our experimental setup. Note how, in the second frame, the snake deforms due to impacts with the pegs to fit the narrow opening and overcome the obstacle. After having been rotated by the pegs, the snake finally reverses its motion to resume locomotion in the initial direction of travel.

IV. Experiments and Discussion

A. Experimental settings

In our experiments, the setup was a wooden board of $230 \times 115\,cm$, on which eight cylindrical pegs $6\,cm$ in diameter were placed in a single line with non-uniform spacings. An overhead camera was used to record the experiments.

The robot used in this work was an hyper-redundant mechanism composed of eighteen identical series-elastic actuated modules [16], each one rotated by ninety degrees with respect to the previous module's axis, to achieve an alternate orientation in the lateral and dorsal plane of the robot. Each module contains an IMU, jointly used to estimate orientation, and a series-elastic element [17] that enables torque sensing. The gait speed, defined by the temporal frequency, was the same for all the trials. The robot was covered with a braided polyester sleeve in order to smooth the snake body, removing sharp edges that could hinder the movement. We started with the full controller (Spatial Frequency and Amplitude) and removed one parameter at a time, up to the open-loop version:

- Ampl. and Sp. Frequency anti-Compliant (AC-SFC)
- Amplitude anti-Compliant (AC)
- Spatial Frequency anti-Compliant (SFC)
- open-loop (OL)

We conducted 21 experiments for each controller: 3 experiments each for 7 different initial positions.

B. Results

Performance was measured in terms of both reliability and time-efficiency. To estimate reliability, we compared controllers by measuring the first opening along the peg row through which the snake successfully passed, as well as the number of failed attempts, i.e., exiting the experiment area without passing through the pegs. The number of opening was counted from the first possible opening inside which the snake could enter. Controllers that resulted in poor locomotion performance either passed through one of the latest openings or failed to pass through. The last openings were made larger to gradually decrease the difficulty associated with overcoming the peg row. To measure time-efficiency, we measured the average time needed for the snake to sidewind through an opening, and complete its reversal maneuver. Figure 2 shows a sequence of frames, as the snake passes through the row of pegs. Videos of all experiment can be found at `https://goo.gl/WbWFCa`.

Figures 3 and 4 present our experimental results. Figure 3 shows the mean of the number of opening passed over by the snake before passing through the pegs and reversing, and the number of failed attempts. Figure 4 shows the average time required by the snake to overcome the row of obstacles, from the initial contact with a peg until the end of the reversal.

C. Discussion

The concept of impact-triggered reflexes, used to facilitate locomotion, can be implemented in different ways on a robot. In this paper we explored three different behaviors, each governed by a specific version of the controller Eq.(3) and (5). The SFC controller is very reliable at the expense of speed; while it fails passing through the pegs only a few times, it is the slowest controller. On the contrary, the AC controller is the most time-efficient, though barely, but has the highest amount of failed attempts, and hence is very unreliable. The AC-SFC controller combines reliability and speed, never failing to pass through and without sacrificing speed. While the OL controller simply moves along the obstacles, the anti-compliant controllers allow the snake to conform its shape to the pegs while propelling forward. Overall, the AC-SFC controller results in a slightly faster locomotion through the obstacles than the OL controller, but is considerably more reliable than all other controllers.

We experimentally demonstrated how a certain degree of flexibility is beneficial for the snake to adapt to different-sized openings between obstacles. Specifically, experiments showed how shape-based anti-compliance improves the ability to get past obstacles. That is, actively pushing against the obstacle allows to stochastically orient the snake toward an opening, while simultaneously providing the necessary force to propel on the pegs and locomote through an opening. This experimentally validates our hypothesis, and highlights the advantages of using positive feedback to react to occasional impacts with the environment.

Finally, during the experiments with the AC-SFC controller, we note that hierarchical control decentralization proves to be beneficial to the snake locomotion. That is, as the centralized spatial frequency parameter allows the body's wavelength to conform to openings' sizes, the decentralized amplitude parameter exerts local forces which propel the snake forward and eventually past the pegs.

V. Extension to Legged Locomotion

The new modular framework for proprioceptive-inertial locomotion introduced in this work can be extended to more general types of locomotion. That is, granting environment-dependent reflexes to an articulated mobile robot is useful for a wide range of self-locomoting behaviors. In particular,

we consider hexapodal locomotion, and detail how anti-compliance can be used to implement a proprioceptive *elevator reflex* [9], [18], allowing a robot to overcome obstacles by increasing its step height.

A. Motion parameterization

In the case of legged locomotion, a shape function for a system is generally not straightforward to define and utilize. That is, such function will depend on the individual shapes of all the limbs, as well as on their interactions during locomotion. Therefore, in such cases, we propose to rely on motion parameterization to adapt locomotion.

In our case, open-loop gait generation for the hexapod relies on an underlying central pattern generator (CPG), which couples the six horizontal shoulder joints of the robot. The rest of the joints, i.e., a vertical shoulder joint and a vertical elbow joint per leg, are coordinated by means of closed-form inverse kinematic equations based on the state of the horizontal shoulder joints. The CPG equation for the horizontal shoulder joints builds on [19], extending it to hexapod locomotion, and considering ellipsoid limit cycles:

$$\begin{cases} \dot{x}_i = -2a\,\omega\,y + \gamma\left(\mu^2 - (bx^2 + ay^2)\right)\cdot 2b\,x \\ \dot{y}_i = +2b\,\omega\,x + \gamma\left(\mu^2 - (bx^2 + ay^2)\right)\cdot 2a\,y + \sum_j k_{ij}\,y_j, \end{cases} \tag{11}$$

where $a, b \in \mathbb{R}$ define the semi-long and semi-short axes of the ellipsoid limit-cycle, $\gamma \in \mathbb{R}^+$ determines the damping toward the limit-cycle. The shape of the limit-cycle reads $b\,x^2 + a\,y^2 = \mu^2$, and for $a = b = 1$, we obtain a circular limit-cycle. $K = (k_{ij})$ is the coupling matrix defining the gait; In our case, we consider the alternate-tripod gait, where

$$K = \begin{pmatrix} 0 & -1 & -1 & 1 & 1 & -1 \\ -1 & 0 & 1 & -1 & -1 & 1 \\ -1 & 1 & 0 & -1 & -1 & 1 \\ 1 & -1 & -1 & 0 & 1 & -1 \\ 1 & -1 & -1 & 1 & 0 & -1 \\ -1 & 1 & 1 & -1 & -1 & 0 \end{pmatrix}. \tag{12}$$

Using Eq.(11), we let $x_i(t)$ control the angles of the horizontal shoulder joints. The values $y_i(t)$ are used to determine if a leg is in stance ($y_i(t) \leq 0$) or in flight ($y_i(t) > 0$). During flight, $y_i(t)$ is also used to determine the step height.

B. Elevator reflex

During locomotion in unstructured and challenging terrains, legged robots must adapt the height of their steps in order to overcome high obstacles. Step height can be adapted by relying on force sensing in the flight legs, by implementing an elevator reflex. This reflex behavior increases the step height as flight legs senses a forward impact, in order to naturally try to climb over an obstacle.

The anti-compliant framework introduced in Section II can be used to implement step height adaptation, by relying on forces sensed at the horizontal shoulder joint. In our case, the step height of leg i is defined as $A_i(t)$, and is used in the inverse kinematics to determine the vertical position $Z_i(t)$ of the end effector of leg i. The position $Z_i(t)$ also depends on the output of the $y_i(t)$ signal of Eq.(11), and reads

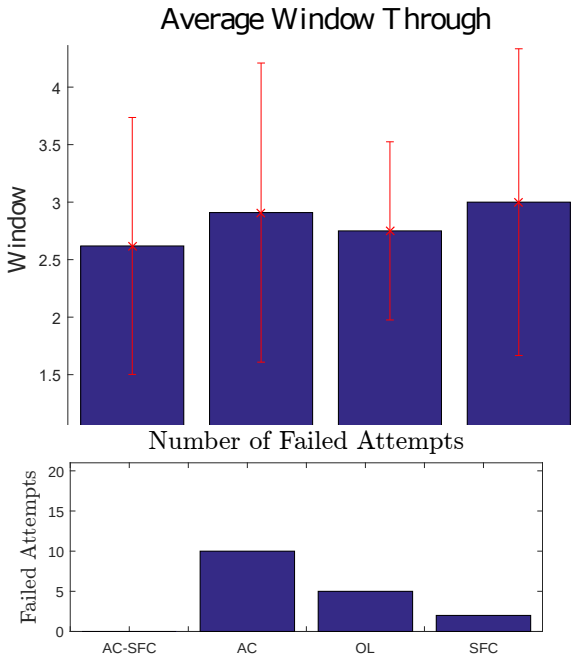

Fig. 3. Top: average number of openings the snake passed by before passing through the row of obstacles. Bottom: number of failed attempts for each controller, out of 21 trials. Red bars indicate the standard deviations.

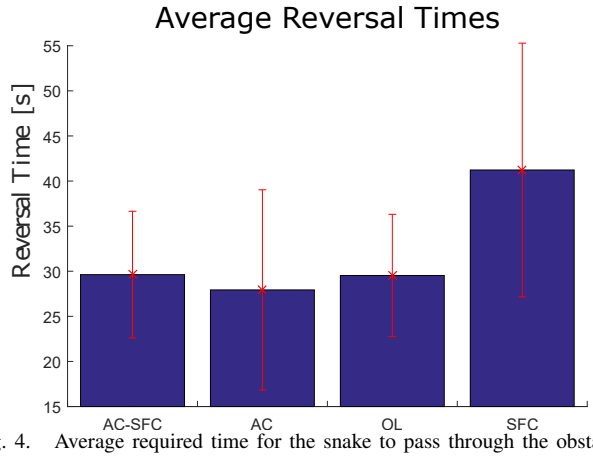

Fig. 4. Average required time for the snake to pass through the obstacle row for each controller, from initial contact with a peg until end of the reversal maneuver. Red bars indicate the standard deviations.

$$Z_i(t) = A_i(t) \cdot \frac{\max(0, y_i(t))}{\mu}. \tag{13}$$

In order to implement a proprioceptive elevator reflex, we let $A_i(t)$ increase in reaction to forward forces. Anti-compliance of the step height is obtained using the admittance controller Eq.(3), with $\beta(t) = A_i(t)$, $\beta_0 = A_{0,i}$. In this controller, the external forcing $F(t)$ reads:

$$F(t) = -J(x_i(t)) \cdot \tau_{ext,i}, \tag{14}$$

where $\tau_{ext,i}$ is the external force sensed by the horizontal shoulder joint i $(i + 1, .., 6)$, and J is the Jacobian matrix associated with the motion parameterization Eq.(11). The Jacobian matrix J expresses how external torques sensed by the shoulder joints translate to forward forces in the robot's body frame, and reads:

$$J(x_i(t)) = \frac{1}{\cos(x_i(t))}. \tag{15}$$

In addition to elevator reflexes for each legs, we propose a backward-propagating mechanism for the step height on each

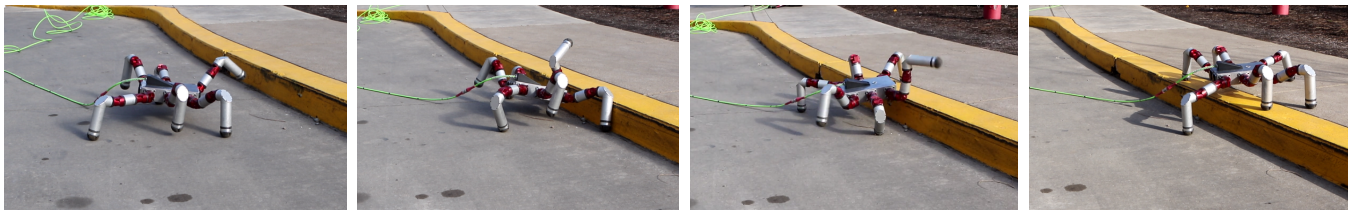

Fig. 5. Sequence of frames of a modular series-elastic hexapod robot climbing a step by relying on a proprioceptive elevator reflex using anti-compliance.

side of the robot. That is, as each leg adapts its individual step height in reaction to external forces, each leg also records the maximal step height $A_{i,j}^{max}$ that was reached by the elevator reflex controller during the flight phase $j \in \mathbb{N}$. This maximal amplitude is then propagated backward to the next leg in line on the same side of the robot, as the nominal step height for its next flight side $A_{0,i+2} = A_{i,j}^{max}$. This mechanism, very similar to the backward-propagation of the amplitude windows along the backbone of the snake robot, allows the hexapod to propagate information sensed by the front legs backwards during forward locomotion. That is, the front legs are effectively used to probe the environment during their flight phases. When an obstacle is detected by one of the front legs, a wave of increased step heights is propagated on the same side of the hexapod, to simplify the climbing.

The CPG-based locomotion Eq.(11), with elevator reflexes Eq.(3),(14) and backward-propagation of the step heights, was implemented on a modular hexapod robot. The hexapod robot is composed of the same series-elastic modules as the snake robot used in Section IV. Each leg is composed of a horizontally-actuated shoulder joint, a vertically-actuated shoulder joint and a vertically-actuated elbow joint. External torques can be measured at each joint.

Figure 5 shows a sequence of frames, as the hexapod adapts its step height upon impact, in order to climb a step of $14\,cm$. Experiments with this controller have been performed indoors and outdoors, on surfaces of varying friction coefficients. Example indoor and outdoor experiments can be found at `https://goo.gl/WbWFCa`.

VI. Conclusion

In this paper, we devised a modular framework for autonomous locomotion of articulated robots, linking relevant parameters of a robot's motion parameterization to proprioceptive and inertial feedback. In doing so, we experimentally demonstrated the performance of anti-compliance when reacting to occasional impacts with unknown and unstructured obstacles. We further experimentally showed how simultaneously relying on various levels of control decentralization can provide structure and improve motion adaptation.

Anti-compliance can be useful when dealing with occasional impacts, whereas evidence shows that compliance improves impact-aided locomotion [3]. Therefore, future works should investigate how to adaptively select between compliant and anti-compliant behaviors during locomotion. Compliance and anti-compliance should also be adapted with respect to the directionality of the forces: external forces in the direction of motion should generally be complied with, while forces in the other direction should be opposed to.

References

[1] H. C. Astley, C. Gong, J. Dai, M. Travers, M. M. Serrano, P. A. Vela, H. Choset, J. R. Mendelson, D. L. Hu, and D. I. Goldman, "Modulation of orthogonal body waves enables high maneuverability in sidewinding locomotion," *Proceedings of the National Academy of Sciences*, vol. 112, no. 19, pp. 6200–6205, 2015.

[2] H. Marvi, C. Gong, N. Gravish, H. Astley, M. Travers, R. L. Hatton, J. R. Mendelson, H. Choset, D. L. Hu, and D. I. Goldman, "Sidewinding with minimal slip: Snake and robot ascent of sandy slopes," *Science*, vol. 346, no. 6206, pp. 224–229, 2014.

[3] M. Travers, J. Whitman, P. Schiebel, D. Goldman, and H. Choset, "Shape-based compliance in locomotion," in *Proceedings of Robotics: Science and Systems*, AnnArbor, Michigan, June 2016.

[4] J. Whitman, F. Ruscelli, M. Travers, and H. Choset, "Shape-based compliant control with variable coordination centralization on a snake robot," in *CDC 2016*, December 2016.

[5] K. E. Cullen, "The vestibular system: multimodal integration and encoding of self-motion for motor control," *Trends in neurosciences*, vol. 35, no. 3, pp. 185–196, 2012.

[6] J. R. Lackner and P. DiZio, "Vestibular, proprioceptive, and haptic contributions to spatial orientation," *Annual Review of Psychology*, vol. 56, pp. 115–147, 2005.

[7] A. Frigon and S. Rossignol, "Experiments and models of sensorimotor interactions during locomotion," *Biological Cybernetics*, vol. 95, no. 6, p. 607, 2006.

[8] P. J. Whelan, "Control of locomotion in the decerebrate cat," *Progress in neurobiology*, vol. 49, no. 5, pp. 481–515, 1996.

[9] K. S. Espenschied, R. D. Quinn, R. D. Beer, and H. J. Chiel, "Biologically based distributed control and local reflexes improve rough terrain locomotion in a hexapod robot," *Robotics and autonomous systems*, vol. 18, no. 1-2, pp. 59–64, 1996.

[10] A. Prochazka, D. Gillard, and D. J. Bennett, "Positive force feedback control of muscles," *Journal of neurophysiology*, vol. 77, no. 6, pp. 3226–3236, 1997.

[11] M. Travers, A. Ansari, and H. Choset, "A dynamical systems approach to obstacle navigation for a series-elastic hexapod robot," in *IEEE Conference on Decision and Control*, December 2016.

[12] M. Tesch, K. Lipkin, I. Brown, R. Hatton, A. Peck, J. Rembisz, and H. Choset, "Parameterized and scripted gaits for modular snake robots," *Advanced Robotics*, vol. 23, no. 9, pp. 1131–1158, 2009.

[13] S. Hirose, *Biologically Inspired Robots: Serpentile Locomotors and Manipulators*. Oxford University Press, 1993.

[14] D. Rollinson and H. Choset, "Gait-based compliant control for snake robots," in *IEEE International Conference on Robotics and Automation*. IEEE, 2013, pp. 5138–5143.

[15] C. Ott, R. Mukherjee, and Y. Nakamura, "Unified impedance and admittance control," in *IEEE International Conference on Robotics and Automation*, 2010, pp. 554–561.

[16] D. Rollinson, Y. Bilgen, B. Brown, F. Enner, S. Ford, C. Layton, J. Rembisz, M. Schwerin, A. Willig, P. Velagapudi, and H. Choset, "Design and architecture of a series elastic snake robot," in *Proceedings of IROS*, 2014, pp. 4630–4636.

[17] G. A. Pratt and M. M. Williamson, "Series elastic actuators," in *IEEE/RSJ International Conference on Intelligent Robots and Systems*, vol. 1. IEEE, 1995, pp. 399–406.

[18] P. Wand, A. Prochazka, and K. H. Sontag, "Neuromuscular responses to gait perturbations in freely moving cats," *Experimental Brain Research*, vol. 38, no. 1, pp. 109–114, 1980.

[19] L. Righetti and A. J. Ijspeert, "Pattern generators with sensory feedback for the control of quadruped locomotion," *IEEE International Conference on Robotics and Automation*, pp. 819–824, 2008.